ISBN: 978-3-95450-231-8 ISSN: 2673-5490 doi: 10.18429/JACoW-IPAC2023-THPA046

OVERVIEW OF THE RADIATION LEVELS IN THE CERN ACCELERATOR COMPLEX AFTER LS2

A. Canesse*, S. Danzeca, D. Di Francesca, R. Garcia Alia, G. Lerner, D. Prelipcean†, D. Ricci, A. Zimmaro, CERN, Geneva, Switzerland

Abstract

The PSB, PS, and SPS accelerators at CERN provide high-energy proton and ion beams to a wide range of experiments, from fixed targets to the world's biggest particle accelerator: the Large Hadron Collider (LHC). In 2021 and 2022, their beams have reached unprecedented intensities thanks to the LHC Injectors Upgrade (LIU) undertaken during the Long Shutdown 2 (LS2) in preparation of the High-Luminosity (HL) LHC era. The operation of these accelerators results in beam losses that generate a mixed radiation field that can negatively impact the exposed electronic systems through cumulative and single event effects. To minimise the associated damage, including potential the machine downtime due to radiation effects on electronics, the evolution and distribution of radiation levels must be carefully monitored across the CERN complex to promptly detect anomalies, to propose mitigation measures to protect electronic systems when needed, and to plan the installation of new electronic systems appropriately. This contribution will give an overview of the new radiation levels across the CERN injector complex in 2021 and 2022.

INTRODUCTION

During operation, particle accelerators produce prompt radiations through two main processes: beam-machine element interactions and beam-gas interactions. The equipment, especially electronic systems, located in the vicinity of accelerators is therefore subjected to the resulting mixed radiation field [1]. All exposed equipment suffers from cumulative radiation effect and electronic systems are also subjected to Single Event Effects (SEE), both potentially leading to premature failures.

To mitigate the radiation-induced machine downtime in the CERN injector complex, it is imperative to accurately monitor radiation levels and take appropriate action. This includes implementing measures such as shielding and relocation to minimize the impact on installed equipment, as well as predicting the evolution of radiation levels to design future equipment accordingly. This is even more important after all the machine changes from the recent injector upgrade [2] that doubled the proton beam intensity that can be delivered to LHC in preparation for the HL-LHC upgrade.

This paper presents an overview of the 2022 radiation levels in the PSB [3], PS [4] and SPS [5] accelerator tunnels, as well as the transfer lines TT41, TT66, TI2 and TI8 leading from the SPS to the AWAKE experiment [6], HiRadMat facility [7] and LHC beam 1 and 2 respectively. Two quantities are monitored: the Total Ionising Dose (TID) and the High Energy Hadron equivalent (HEH-eq) Fluence. The 2022 data is also compared to 2021 levels to look for differences.

DATA ACQUISITION

An automated radiation analysis system [8] has been put in place to process and monitor the radiation levels measured in the tunnels by three types of detectors: Beam Loss Monitors (BLM), Distributed Optical Fiber Radiation Sensing (DOFRS), and Radiation Monitoring System (RadMon) which are described below. Additionally, in first approximation and for constant machine settings, radiation losses are known to scale with injected beam intensity, which is measured by Beam Current Transformers (BCT). The annual post-LS2 injected intensities are shown in Table 1.

Table 1: Total Number of Charges (Proton and Ion) Injected into the Different CERN Accelerators in 2021 and 2022 and the 2022/2021 Ratio

	2021 (charges)	2022 (charges)	ratio
PSB	1.18e+20	1.75e+20	1.48
PS	2.94e+19	6.25e+19	2.13
SPS	1.17e+19	2.43e+19	2.07

Beam Loss Monitor

Beam Loss Monitors are ionisation chamber detectors filled with N_2 gas that were originally developed for machine protection at CERN [9]. They are installed close to the beamline of all injection accelerators and can withstand up to 10^8 Gy, covering a high dynamic range of over 10^9 with a fast time response of only dozens of microseconds. With careful analysis, they can be used for dosimetry to measure Total Ionizing Dose (TID).

DOFRS

The DOFRS [10] system uses a set of silica based radiation sensitive optical fibers deployed along the accelerators tunnels walls at constant distance from the beam-pipe, and an optical time domain reflectometer (OTDR) to periodically measure the Radiation Induced Attenuation (RIA) of the fiber. The laser pulses used in this study are 10 ns long and have a wavelength of 1625 nm, which allows a TID(Si) measurement with ~2-m spatial resolution.

RadMon

The RadMon System, is specifically designed to measure radiation levels of complex environments and assess

* auriane.canesse@cern.ch
† Presenter

ISBN: 978-3-95450-231-8 ISSN: 2673-5490 doi: 10.18429/JACoW-IPAC2023-THPA046

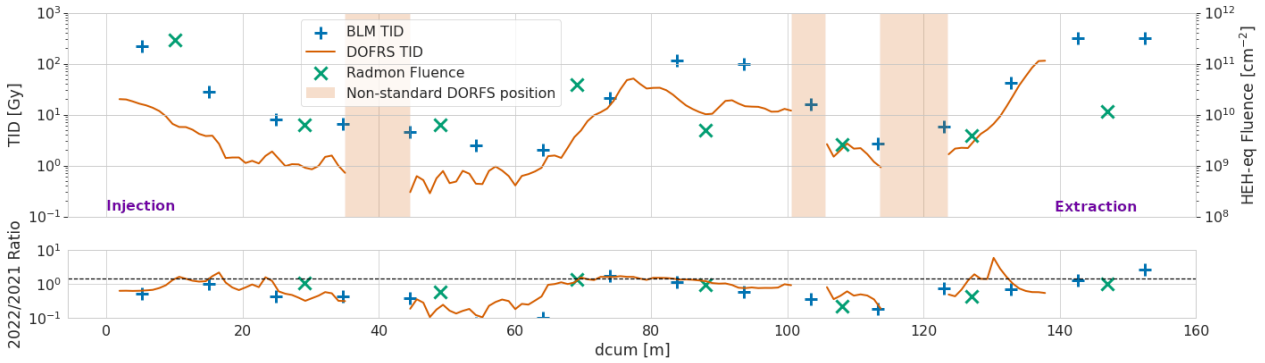

Figure 1: Radiations levels in the PSB tunnel as a function of position in 2022 (top), measured with different detectors. Ratio of radiation levels between 2022 and 2021 for comparison (bottom).

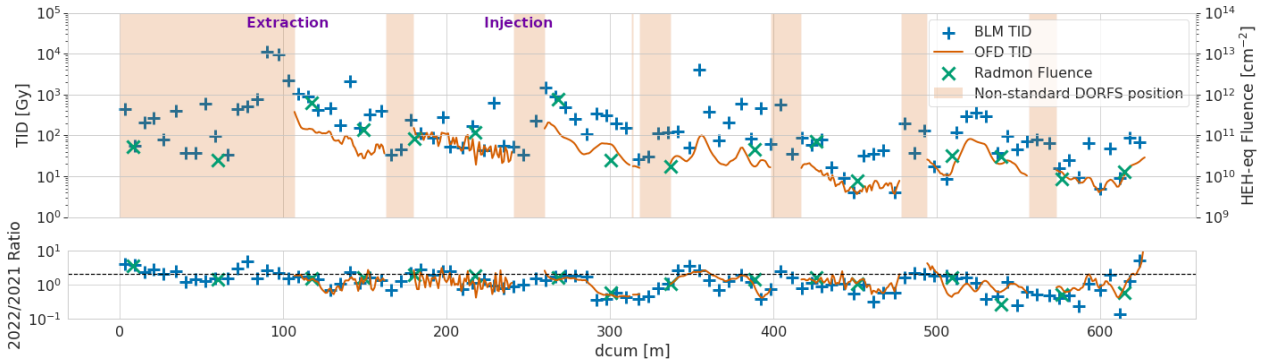

Figure 2: Radiations levels in the PS tunnel as a function of position in 2022 (top), measured with different detectors. Ratio of radiation levels between 2022 and 2021 for comparison (bottom).

its impact on electronic systems [11]. RadMon monitors utilise Radiation-sensing Field-Effect Transistors (RadFETs) to measure the Total Ionizing Dose (TID) in Silicon dioxide, p-i-n diodes to gauge the Displacement Damage (DD) in Silicon, and counts Single Events Upsets (SEU) in SRAM memory to determine the High Energy Hadrons equivalent (HEH-eq) and thermal neutrons fluences. The RadMons considered here are located at the floor level below the accelerator's magnets and are less exposed to radiation than the BLMs.

RESULTS

For each accelerator, 2022 radiation levels are presented as a function of the Distance CUMulated (dcum) along the machine, and then compared to 2021 data (ratio plots). DORFS data is presented for the areas in which the fibre is in standard position, i.e., running along the tunnel on a cable tray at a fixed distance from the accelerator. The injected intensity ratio values are shown in black. The maximum radiation levels for each machine are summarised in Table 2.

PSB

The radiation levels in the PSB tunnel are shown in Fig. 1. The highest TID measured (433 Gy) is located around dcum 140 m which corresponds to PSB periods 15-16 (extraction). A TID of 116-96 Gy was recorded around dcum 83-93 m (periods 8-9) and good agreement is observed in the TID distribution measured by both DORFS and BLMs. The HEH-eq fluence distribution is in good agreement with TID measurements and varies from 2.94 10^{11} cm^{-2} (period 15-16) to 2.60 10^{9} cm^{-2} (period 5-6).

PS

The radiation levels in the PS tunnel are shown in Fig. 2. The highest TID measured (9.39 10^{3}-1.14 10^{4} Gy) is located around dcum 90-97 m which corresponds to PS cells 15-16 (extraction to SPS). Good agreement is observed in the TID distribution measured by both DORFS and BLMs. No RadMon is present at the the beam extraction, therefore the maximum HEH-eq fluence is measured at 7.54 10^{11} cm^{-2} (dcum 268 m, cell 43, close to PSB injection) and the lowest values is 7.89 10^{9} cm^{-2} measured at dcum 451 m (cell 72).

SPS

The maximum radiation levels per SPS sextant are shown in Table 2. The highest radiation levels (3.06 10^{5} Gy) are reached in LSS2 where the beam is extracted to the North Area. The radiation levels in the SPS sextant 2 tunnel are shown in Fig. 3. Note that due to the high radiations reached in LSS2, part of the DORFS data could not be readout

ISBN: 978-3-95450-231-8 ISSN: 2673-5490 doi: 10.18429/JACoW-IPAC2023-THPA046

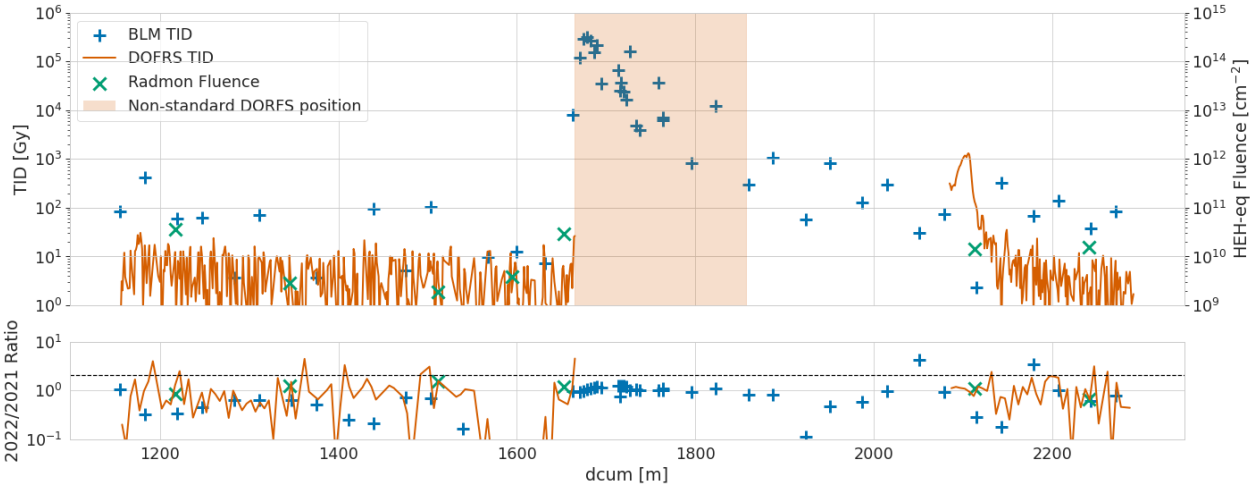

Figure 3: Radiations levels in the sector 2 of the SPS tunnel as a function of position in 2022 (top). Ratio of radiation levels between 2022 and 2021 for comparison (bottom). Due to its higher radiation hardness (compared to PSB and PS), the DOFRS used for the SPS cannot resolve to doses below ~10 Gy.

until the end of the year. The RadMons do not cover the area either. HEH-eq Fluence levels in the SPS varies from 3.77 10^{11} cm^{-2} (sextant 6, cell 34) to 5.62 10^{8} cm^{-2} (sextant , cell 6). A more detailed analysis of SPS radiation levels can be found in [12].

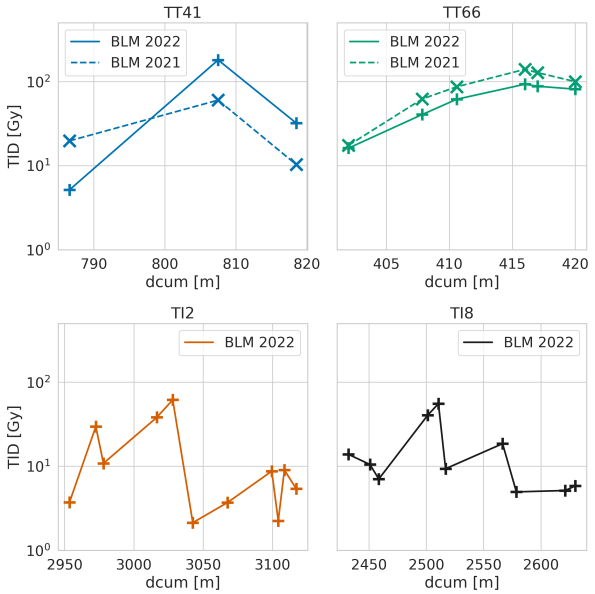

Figure 4: Transfer lines TID levels for locations above 1 Gy.

Transfer Lines

Only BLM data in the transfer lines. Most of the yearly measurements were below 1 Gy and only the areas above that threshold are shown in Fig. 4. For TT41 the dcum 800-820 m corresponds to the AWAKE experiment [6], the end of TT66 is where the HiRadMat target & beam dump are located, and finally the end of TI2 and TI8 are the extractions to the LHC. Note that 2021 is not shown for TI2 & TI8 as negligible beam intensities were sent to LHC.

Table 2: Maximum annual radiation levels measured for each accelerator and transfer line. Due to its size the, the SPS values are given for each sextant (1-6). Note that RadMons cannot operate in the highest radiation zones and higher HEH-eq fluence could be reached in non-monitored areas.

	TID [kGy]		HEH-eq Fluence [cm^{-2}]	
	2021	2022	2021	2022
PSB	4.33 10^{-1}	3.14 10^{-1}	2.97 10^{10}	2.94 10^{11}
PS	4.38 10^{0}	1.14 10^{1}	4.54 10^{11}	7.54 10^{11}
SPS-1	3.73 10^{1}	5.19 10^{1}	1.31 10^{11}	1.18 10^{11}
SPS-2	3.06 10^{2}	3.24 10^{2}	5.52 10^{11}	3.64 10^{10}
SPS-3	2.97 10^{0}	1.75 10^{0}	4.12 10^{10}	5.90 10^{10}
SPS-4	1.03 10^{0}	2.16 10^{0}	2.40 10^{10}	3.16 10^{10}
SPS-5	4.14 10^{0}	3.15 10^{0}	4.30 10^{10}	3.95 10^{10}
SPS-6	2.38 10^{0}	1.77 10^{0}	2.47 10^{11}	3.77 10^{11}
TT40	6.02 10^{-2}	1.81 10^{-1}	N/A	N/A
TT60	1.40 10^{-1}	9.31 10^{-2}	N/A	N/A
TI2	5.02 10^{-4}	6.19 10^{-2}	N/A	N/A
TI8	6.57 10^{-4}	5.56 10^{-2}	N/A	N/A

CONCLUSION

Radiation levels have been measured 2022 in the PSB, PS, SPS tunnels and transfer lines TT41, TT66, TI2 & TI8. Good agreement in the radiation level distribution is observed between the different monitors. Their complementarity allows a details mapping of the radiation fields across the CERN injector complex covering a dynamic range from 1 to 10^{5} Gy and 10^{7} to 10^{11} cm^{-2} HEH-eq Fluence. While local exceptions can be found, the radiation levels have generally increased from 2021 to 2022 consistently with what is expected from injected intensity scaling.

ISBN: 978-3-95450-231-8 ISSN: 2673-5490 doi: 10.18429/JACoW-IPAC2023-THPA046

REFERENCES

[1] S. De Carvalho *et al.*, "Radiation Environments and their Impact at the CERN's Injector Chain" CERN, Geneva, Switzerland, Rep. CERN-ACC-NOTE-2015-0042, Dec. 2015. https://cds.cern.ch/record/2114889

[2] H. Damerau *et al.*, "LHC Injectors Upgrade, Technical Design Report: Vol I", CERN, Geneva, Switzerland, Rep. CERN–ACC–2014-0337, Dec. 2014. doi:10.17181/CERN.7NHR.6HGC

[3] J. Burnet *et al.*, "Fifty years of the CERN Proton Synchrotron: Volume I", CERN, Geneva, Switzerland, Rep. CERN-2011-004, Jun. 2011. doi:10.5170/CERN-2011-004

[4] J. Burnet *et al.*, "Fifty years of the CERN Proton Synchrotron: Volume II", CERN, Geneva, Switzerland, Rep. CERN-2013-005, Aug. 2013. doi:10.48550/arXiv.1309.6923

[5] P. Collier *et al.*, "The SPS as Injector for LHC: Conceptual Design", CERN, Geneva, Switzerland, Rep. CERN-SL-97-007-DI, Mar. 1997.

[6] A. Caldwell *et al.*, "AWAKE Design Report: A Proton-Driven Plasma Wakefield Acceleration Experiment at CERN", CERN, Geneva, Switzerland, Rep. CERN-SPSC-2013-013, SPSC-TDR-003, Sep. 2013. https://cds.cern.ch/record/1537318

[7] "The HiRadMat Facility at SPS", https://hiradmat.web.cern.ch/.

[8] K. Biłko, R. García Alía, and J. B. Potoine, "Automated Analysis of the Prompt Radiation Levels in the CERN Accelerator Complex", in *Proc. IPAC'22*, Bangkok, Thailand, Jun. 2022, pp. 736–739. doi:10.18429/JACoW-IPAC2022-MOPOMS043

[9] B. Dehning *et al.*, "The LHC Beam Loss Measurement System", in *Proc. PAC'07*, Albuquerque, NM, USA, Jun. 2007, paper FRPMN071, pp. 4192–4194. https://jacow.org/p07/papers/FRPMN071.pdf

[10] D. Di Francesca *et al.*, "Dosimetry Mapping of Mixed-Field Radiation Environment Through Combined Distributed Optical Fiber Sensing and FLUKA Simulation", *IEEE Trans. Nucl. Sci.*, vol. 66, no. 1, pp. 299–305, Jan. 2019. doi:10.1109/TNS.2018.2882135

[11] G. Spiezia *et al.*, "A new RadMon version for the LHC and its injection lines", *IEEE Trans. Nucl. Sci.*, vol. 61, no. 6, pp. 3424–3431, Dec. 2014. doi:10.1109/TNS.2014.2365046

[12] K. Biłko *et al.*, "CERN Super Proton Synchrotron radiation environment and related Radiation Hardness Assurance implications", *IEEE Trans. Nucl. Sci.*, Mar. 2023. doi:10.1109/TNS.2023.3261181